Structural Investigations on Smectic Blue Phases

Eric Grelet,[1] Brigitte Pansu,[1] Min-Hui Li,[2] and Huu Tinh Nguyen[3]

[1]*Laboratoire de Physique des Solides, UMR 8502, Université Paris-Sud, F-91405 Orsay Cedex, France*
[2]*Institut Curie-Section de Recherche, UMR 168, 11 rue Pierre et Marie Curie, F-75231 Paris Cedex 05, France*
[3]*Centre de Recherche Paul Pascal, UPR 8641, Avenue Albert Schweitzer, F-33600 Pessac, France*

(Received 19 October 2000)

Smectic blue phases (BP_{Sm}) are thermotropic liquid crystalline phases which exhibit both three-dimensional orientational order, such as classical blue phases, and smectic positional order. BP_{Sm} appear as the three-dimensional counterpart of twist grain boundary phases. X-ray scattering and optical polarizing microscopy provide information on the hexagonal and cubic symmetries of these new phases.

DOI: 10.1103/PhysRevLett.86.3791 PACS numbers: 61.30.Eb, 61.10.–i

Liquid crystals are intermediate states of condensed matter that combine long-range positional or orientational order along some directions of space and liquidlike order along at least one of the other directions. When the molecules are chiral, a spontaneous twist of the molecular orientation occurs. But this local orientational order can induce frustration and therefore complex structures sometimes occur. For instance, a high chirality can generate original mesophases between the cholesteric phase and the isotropic one: the blue phases (BP) [1]. Two of these blue phases, BP1 and BP2, exhibit an unusual cubic symmetry in which the orientational (but not positional) order is periodic and long range in three dimensions. The third blue phase, called BP3, seems to have an amorphous structure of the same macroscopic symmetry as that of the isotropic phase [2]. The blue phase structures involve a twist of the director (average molecular orientation) extending not only in one direction, such as in the cholesteric phase, but in both directions perpendicular to the director, called double twist. This double twist cannot perfectly extend in the three-dimensional space. Geometrical models of BP1 and BP2 consist of cubic networks of double twist cylinders, separated by defect lines. Thus blue phases can also be seen as a periodic array of disclination lines. A second example of a frustrated chiral system is the twist grain boundary (or TGB) phases predicted by Renn and Lubensky [3]. Indeed, the smectic layers in the smectic *A* phase cannot be continuously twisted. TGB phases are made by slabs of a smectic material, which are regularly stacked in a helical fashion along an axis parallel to the smectic layers. Adjacent slabs are continuously connected via a grain boundary which consists of a wall of parallel equidistant screw dislocation lines allowing helical twist. In these phases, the frustration is also relieved by the presence of defects. TGB phases have been experimentally found in chiral thermotropic liquid crystals by Goodby *et al.* in 1989 for TGB_A [4] and by Nguyen *et al.* in 1992 for TGB_C [5].

Recently new phases have been discovered in a chiral material (called FH/FH/HH-*n*BTMHC where *n* indicates the paraffinic chain length) with the following phase sequence: TGB phases–BP–Iso [6]. In this sequence, three blue phases appear between the isotropic phase and the TGB_A phase without any intermediate cholesteric state for all the compounds with $14 \leq n \leq 18$. Contrary to classical blue phases, these phases, called smectic blue phases (BP_{Sm}), exhibit quasi-long-range smectic order, that can then be studied by x-ray scattering. The smectic order is correlated with the orientational three-dimensional order and is therefore enhanced in some directions. These smectic peaks give information on the symmetry of the BP_{Sm} unit cell. Indeed, the BP_{Sm} lattice parameter is in the UV range [6], preventing any optical scattering of visible light (Kossel diagram technique), which is commonly used to find the symmetry of classical blue phases [7]. We have recently found the structure of the first smectic blue phase, $BP_{Sm}2$, which shows hexagonal symmetry [8]. This study has been mainly carried out by x-ray scattering on $BP_{Sm}2$ monodomains, grown *in situ* from the isotropic $BP_{Sm}3$. The evidence of hexagonal as opposed to cubic symmetry proves that smectic blue phases are really new phases, and are not merely classical blue phases with smectic fluctuations. Thus smectic blue phases are original physical systems with a double frustration: the extension of the chirality in the three spatial dimensions like classical blue phases, and the helical twist competing with smectic order, as happens for TGB phases. However the determination of the whole phase diagram remained an open question, especially the symmetry of the $BP_{Sm}1$ phase. Monodomains must be grown to determine $BP_{Sm}1$ structure. For classical blue phases, several orientations of BP1 are usually obtained from one BP2 monodomain, illustrated under the microscope by "crosshatching" in the BP texture [1]. Thus single BP1 monodomains cannot be nucleated if BP2 is present in the phase diagram. Such monodomains have been obtained in samples presenting a direct transition from BP3 to BP1. Indeed BP2 can disappear in the phase diagram by decreasing the chirality, for instance by adding controlled amounts of enantiomers [9]. But, contrary to classical blue phases, $BP_{Sm}1$ first disappears when decreasing the chirality [10]. It seems then impossible to obtain a direct transition from $BP_{Sm}3$ to $BP_{Sm}1$. In this Letter, we report two ways of growing monodomains of $BP_{Sm}1$. Contrary to classical blue phases, the growth of $BP_{Sm}1$

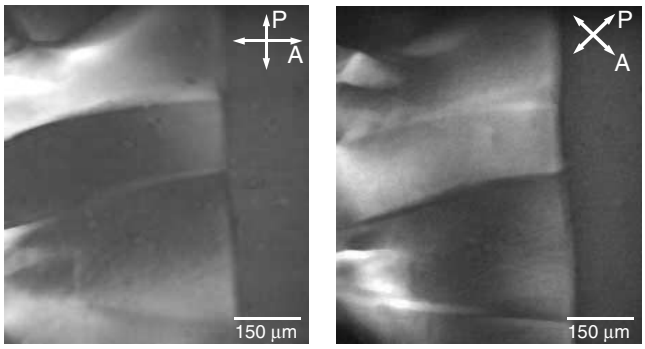

FIG. 1. Single $BP_{Sm}1$ monodomains grown from the $BP_{Sm}3$ phase (dark background) seen by transmission between crossed polarizers: a weak birefringence is observed. The platelets of $BP_{Sm}1$ appear blue due to their optical activity. The sample thickness is 100 μm.

monodomains directly from the $BP_{Sm}2$ phase is possible using a very low cooling rate. The second way consists of nucleating $BP_{Sm}1$ from the isotropic $BP_{Sm}3$ phase by playing with the metastability of $BP_{Sm}3$. The structural studies of $BP_{Sm}1$ monodomains will be presented and $BP_{Sm}1$ orientational symmetry will then be discussed. In particular, we will determine for the first time the symmetries of all BP_{Sm} phases occurring in the phase diagram.

Up to now, all structural investigations on BP_{Sm} have been done on the compound FH/FH/HH-nBTMHC with $n = 18$ [8,11]. Systematic studies of these molecules, varying only the paraffinic chain length n, show that for $n = 14$, $BP_{Sm}3$ can be metastable in the temperature range of $BP_{Sm}2$. Indeed three smectic blue phases have been observed with FH/FH/HH-**14**BTMHC: $BP_{Sm}3$ between 74.4 and 73.2 °C, $BP_{Sm}2$ between 73.2 and 72.3 °C, and $BP_{Sm}1$ between 72.3 and 72.1 °C (upon cooling) [6]. However, fast cooling (typically $\geq$0.5 °C/min) from the isotropic phase (or $BP_{Sm}3$) to the temperature range of $BP_{Sm}2$ can induce the metastability of $BP_{Sm}3$, i.e., $BP_{Sm}2$ does not nucleate in its stability temperature range. Therefore, the nucleation and growth of single $BP_{Sm}1$ monodomains can take place by cooling the supercooled $BP_{Sm}3$ phase with a low rate (0.01 °C per 10 min). This nucleation process, called (a) can be summarized with

$$\text{Iso or } BP_{Sm}3 \xrightarrow[1\,^\circ\text{C/min}]{} \text{metastable } BP_{Sm}3 \xrightarrow[0.01\,^\circ\text{C/10 min.}]{} BP_{Sm}1$$

Thus, this method produces single $BP_{Sm}1$ monodomains in the isotropic $BP_{Sm}3$ phase (Fig. 1), and avoids nucleating the $BP_{Sm}1$ phase from $BP_{Sm}2$ crystallites. Nevertheless we also succeeded in growing monodomains of $BP_{Sm}1$ from $BP_{Sm}2$ monodomains using a slow cooling rate (typically 0.01 °C per 5 or 10 min). This defines a second nucleation process, called (b), to obtain $BP_{Sm}1$ induced from $BP_{Sm}2$:

$$\text{Iso or } BP_{Sm}3 \xrightarrow[0.01\,^\circ\text{C/10 min}]{} BP_{Sm}2 \xrightarrow[0.01\,^\circ\text{C/10 min.}]{} BP_{Sm}1$$

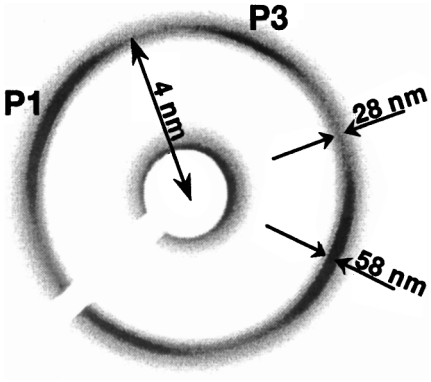

FIG. 2. Experimental x-ray scattering pattern obtained for a single $BP_{Sm}1$ monodomain at $\theta = -10°$. θ is defined by Fig. 3. The monodomain was grown with $\theta = 0$ along the x-ray beam. This scan corresponds roughly to the maximum intensity of the P1 smectic peak (Table I). Because of its angular extension, the P3 smectic peak is also visible on this pattern.

X-ray scattering studies on this compound have been performed. Such studies provide information on the order at the molecular level, as reported in previous works [8,11]. We succeeded in growing $BP_{Sm}1$ monodomains using the two different experimental processes, (a) and (b), as explained above. Kinetics plays an important role in the growth of smectic blue phases with the FH/FH/HH-**14**BTMHC compound: waiting a few hours after slow cooling is necessary to produce a large single monodomain, which then fills the experimental cell. The scattering patterns obtained with the monodomains of both $BP_{Sm}1$ and $BP_{Sm}2$ exhibit pairs of peaks indicating that the smectic order is not isotropic, but extends in given directions of the three-dimensional unit cell (Fig. 2). Note that these peaks have a wide angular extension; we will characterize them in the following by the position of their maximum intensity. The correlation length ζ defined as $\zeta = 2\pi/\text{FWHM}$ (full width at half maximum), associated with the smectic order, has been estimated to be typically 58 nm for both $BP_{Sm}1$ and $BP_{Sm}2$ smectic peaks. For the smectic background of the scattering ring, ζ increases from 19 nm for $BP_{Sm}2$ to 28 nm for $BP_{Sm}1$ (Fig. 2). With the experimental setup we used in these

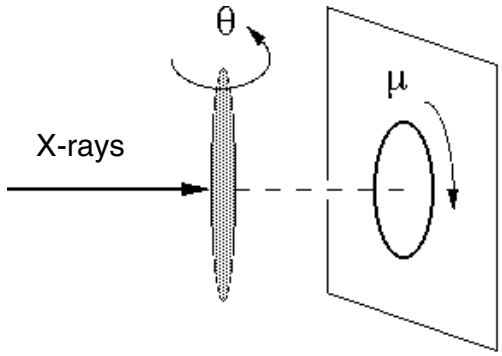

FIG. 3. Schematic representation of the x-ray scattering conditions.

TABLE I. Positions of the three smectic peaks for a $BP_{Sm}1$ monodomain grown from the $BP_{Sm}3$ (P1, P2, P3) or from $BP_{Sm}2$ (PI, PII, PIII). μ is the angle with the vertical axis. θ is the rotation angle around this axis (see Fig. 3). The monodomain was grown with $\theta = 0$ along the x-ray beam. The angles are given in degrees.

	P1 (PI)	P2 (PII)	P3 (PIII)
θ	−15 (−20)	62 (−31)	−69 (60)
μ	114 (−14)	65 (76)	36 (88)

x-ray scattering experiments, the FH/FH/HH-**14**BTMHC compound is contained in a glass capillary tube (1 mm diameter) placed vertically inside a hot stage. The sample can be rotated around its main axis to explore the entire reciprocal space (Fig. 3). Once the monodomain is grown, different scattering patterns are recorded on imaging plates by rotating the capillary by steps of 10° between two scans. Let us call this rotation angle θ. The intensity $I(\theta, \mu)$ along the ring has been analyzed as a function of the angle, μ, with the vertical axis (Fig. 3). Then, by combining these various profiles, we can determine the directions of smectic order enhancement, i.e., where the different smectic peaks are located (Tables I and III) and then deduce the angles between these peaks (Tables II and IV). It is important to note here that the Bragg scattering is not due to the periodicity of the orientational order. Indeed, we detect the Fourier transform of some pattern in the unit cell linked to a periodicity of about 4 nm (Fig. 2) that is the smectic order. Nevertheless, the symmetries exhibited by these patterns certainly reflect those of the three-dimensional unit cell of these phases.

The results of the exploration of the reciprocal space of a $BP_{Sm}1$ monodomain grown from $BP_{Sm}3$ (a) or from $BP_{Sm}2$ (b) are the same: we observe three pairs of smectic peaks perpendicular to each other (Table II, Fig. 4). This shows that quasi-long-range smectic order is observed along three perpendicular directions, noted P1, P2, P3 for the nucleation process (a) and noted PI, PII, PIII for the nucleation process (b). If the $BP_{Sm}1$ symmetry is similar in both cases, (a) and (b), it is then interesting to follow the evolution of the three-dimensional smectic order symmetry between $BP_{Sm}2$ and $BP_{Sm}1$. The $BP_{Sm}2$ monodomain grown with process (b) exhibits four pairs of peaks (Table III) showing a hexagonal structure (Fig. 4): T1 is perpendicular to the three others peaks (T2, T3, T4), which are separated by angles around 120° (Table IV). Then, a temperature decrease induces the transition of the liquid crystal into $BP_{Sm}1$. Two smectic peaks remain unchanged during the transition and are thus common to $BP_{Sm}2$ and $BP_{Sm}1$: PI ≡ T1 and PII ≡ T2. However, the $BP_{Sm}1$ third peak, labeled PIII, can be considered as the merging of T3 and T4 found in $BP_{Sm}2$ (Tables I and III). Indeed, PIII is located along the bisecting line of T3 and T4. Figure 4 summarizes the transition between $BP_{Sm}2$ and $BP_{Sm}1$, indicating the evolution from a hexagonal symmetry to a cubic one, in terms of the directions where smectic order is enhanced.

TABLE II. Angles (in degrees) between the directions along which the smectic peaks are observed on a $BP_{Sm}1$ monodomain grown from $BP_{Sm}3$ (P1, P2, P3) or from $BP_{Sm}2$ (PI, PII, PIII).

	P1 (PI)	P2 (PII)	P3(PIII)
P1 (PI)	0	90 (91)	90 (91)
P2 (PII)	90 (91)	0	91 (90)
P3 (PIII)	90 (91)	91 (90)	0

TABLE III. Positions of the four smectic peaks T1, T2, T3, T4 for a $BP_{Sm}2$ monodomain (angles in degrees).

	T1	T2	T3	T4
θ	−20	−31	32	90
μ	−15	76	81	97

A first approach for combining smectic order with three-dimensional orientational order has been proposed by Kamien [12] in terms of smectic double twist cylinders. Our experimental results can be easily interpreted from this geometrical model by assuming that the regions where the smectic order can easily extend, corresponding to the peaks, are the smectic double twist cylinder cores. Indeed, in the annular and concentric domains wrapping around this perfect smectic core, the smectic layers are distorted by the twist. A geometrical model of the structure of smectic blue phases can be sketched by packing these smectic double twist cylinders with respect to the observed symmetries [8,12]. The $BP_{Sm}1$ lattice composed of three perpendicular "smectic directions" can fit with three symmetries: cubic, tetragonal, or orthorhombic. However the features of the three pairs of smectic peaks, in terms of intensity and full width at half maximum, are quite similar for the $BP_{Sm}1$ monodomains. Therefore the x-ray patterns suggest that the $BP_{Sm}1$ symmetry is cubic, or almost cubic. We have also studied the smectic blue phases using polarizing microscopy to provide information at macroscopic scale. Their textures observed between crossed polarizers seem similar to those of classical blue phases: a mosaic texture composed of platelets. However, these platelets are clearly birefringent for the hexagonal $BP_{Sm}2$ whereas single $BP_{Sm}1$ monodomains only exhibit a much weaker birefringence (Fig. 1). Note that $BP_{Sm}1$ platelets appear mainly blue due to their optical activity and that selective reflections cannot be seen because

TABLE IV. Angles (in degrees) between the directions along which the smectic peaks are observed for the $BP_{Sm}2$ monodomain.

	T1	T2	T3	T4
T1	0	90	90	92
T2	90	0	118	122
T3	90	118	0	120
T4	92	122	120	0

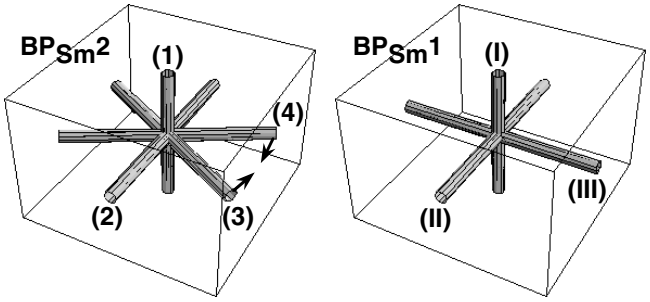

FIG. 4. Geometrical view indicating the directions where the smectic order is enhanced, corresponding to the smectic peaks, for $BP_{Sm}2$ and $BP_{Sm}1$ monodomains. The arrows show their evolution during the transition between the two smectic blue phases.

the lattice parameter is too small, in the near UV range [6]. Using a Berek compensator to measure the optical anisotropy Δn of several sample platelets, we estimate that Δn is around 0.0019 for $BP_{Sm}2$ and 0.0002 or less for $BP_{Sm}1$. Thus the birefringence observed on $BP_{Sm}1$ is 1 order of magnitude smaller than for $BP_{Sm}2$. This optical anisotropy may be intrinsic: the birefringence may originate from the $BP_{Sm}1$ tetragonal (or orthorhombic) structure. Another interpretation is that $BP_{Sm}1$ symmetry is actually cubic and the origin of the birefringence must be explained in another way. Let us note that classical cubic blue phases can exhibit some birefringence as already observed [13]. This low birefringence could be due to local strains induced by the glass surfaces of the cell, by thermal stresses, or mechanical stresses between different platelets. Another source of birefringence is the existence of Bragg reflections in the UV range, thus close to the blue wavelength, which can disturb the optical appearance of theses phases [14]. This effect is similar to the phenomenon of spatial dispersion which makes even cubic crystals birefringent [15]. Therefore, the experimental results presented in this Letter, that is three almost identical and perpendicular smectic peaks and only a very weak birefringence, lead us to conclude that the orientational symmetry of the $BP_{Sm}1$ phase is cubic.

As classical blue phases can be seen as the three-dimensional counterpart of the cholesteric phase, smectic blue phases can be pictured as the extension to 3D of the TGB phase. Indeed, contrary to the cholesteric and to the blue phases where the twist occurs at the "molecular level," the twist occurs at the scale of the smectic slabs for both TGB and smectic blue phases. We have reported here the orientational symmetries of the smectic blue phases, cubic for $BP_{Sm}1$ and hexagonal for $BP_{Sm}2$, which drive their phase diagram. It is interesting to note that an applied electric field can also induce tetragonal and hexagonal symmetries in the phase diagram of classical blue phases [16]. To describe these effects, Landau–de Gennes theory [17] is required using the dielectric tensor as the order parameter and its coupling with the electric field. This work should then stimulate theoretical investigations to find an appropriate coupling between the dielectric tensor and the smectic order parameter, which has to be introduced to predict the whole phase diagram of these new phases.

We would like to thank all the people, especially P. Davidson, who have carefully read the manuscript, V. Dmitrienko for helpful comments, and P.-A. Albouy for the use of his rotating anode generator. We very much appreciate the help of I. Dozov for the birefringence measurements, and of J. Doucet and D. Durand on the D43 synchrotron beam line at LURE where many x-ray scattering experiments were performed.

[1] H. Stegemeyer *et al.,* Liq. Cryst. **1**, 3 (1986).
[2] Z. Kutnjak, C. W. Garland, J. L. Passmore, and P. J. Collings, Phys. Rev. Lett. **74**, 4859 (1995).
[3] S. R. Renn and T. C. Lubensky, Phys. Rev. A **38**, 2132 (1988).
[4] J. W. Goodby *et al.,* Nature (London) **337**, 449 (1989).
[5] H. T. Nguyen *et al.,* J. Phys. II (France) **2**, 1889 (1992).
[6] M. H. Li *et al.,* Liq. Cryst. **23**, 389 (1997).
[7] P. E. Cladis, T. Garel, and P. Pieranski, Phys. Rev. Lett. **57**, 2841 (1986).
[8] B. Pansu, E. Grelet, M. H. Li, and H. T. Nguyen, Phys. Rev. E **62**, 658 (2000).
[9] M. B. Bowling, P. J. Collings, C. J. Booth, and J. W. Goodby, Phys. Rev. E **48**, 4113 (1993).
[10] P. Jamée *et al.,* Phys. Rev. E **62**, 3687 (2000).
[11] B. Pansu, M. H. Li, and H. T. Nguyen, Eur. Phys. J. B **2**, 143 (1998).
[12] R. Kamien, J. Phys. II (France) **7**, 743 (1997).
[13] A. J. Nicastro and P. H. Keyes, Phys. Rev. A **27**, 431 (1983).
[14] V. A. Belyakov and V. E. Dmitrienko, Sov. Sci. Rev. A, Phys. Rev. **13**, 1 (1989).
[15] E. Demikhov and H. Stegemeyer, Liq. Cryst. **14**, 1801 (1993).
[16] H. S. Kitzerow, Mol. Cryst. Liq. Cryst. **202**, 51 (1991).
[17] J. Englert, L. Longa, H. Stark, and H.-R. Trebin, Phys. Rev. Lett. **81**, 1457 (1998).